

Signal Discrimination Based on Power Spectrum of Filter Response

Joni-Kristian Kamarainen*, Ville Kyrki* and Tuomo Lindh†

1 Introduction

In this report, new methods are presented for discrimination of signals. Methods to select Gabor filter parameters are introduced for the discrimination of signals belonging to two different classes. The difference between classes is initially unknown, and feature extraction should be applied prior to classification. In this study an assumption is made that the signals from the two classes have dissimilar frequency content on some frequency band. In such a case, a bandpass filter can be used as the feature extractor but an obvious problem arises: How to select filtering parameters, such as central frequency of filter and bandpass bandwidth. In the presented method the selection is based on first- and second-order statistics of the power spectrum of the filter response. Statistical discrimination energy functions are derived and by maximizing the energy functions the optimal parameters are iteratively searched using gradient information.

2 Features providing discriminative information

In this section, features providing sufficient discriminative information are proposed based on assumptions of the given problem.

There are signals representing two classes, namely class C_1 and class C_2 . The classes can represent, for example, vibration signal measurements made with normal motors and motors containing faults and it is desired to classify signals as accurately as possible to either of these two classes. Let us say that there are N_1 signals representing class C_1 as $x_k(t)$, $k = 0 \dots N_1 - 1$ and N_2 signals representing the class C_2 as $y_k(t)$, $k = 0 \dots N_2 - 1$. It is assumed that the discriminative information is present at some frequency band where the behavior between the two type of signals is measurably different. Due to the assumption it is sufficient to use a bandpass filter $\psi(t)$ and the two classes can be distinguished based on the filter responses calculated using convolutions $\psi(t) * x_k(t)$ and $\psi(t) * y_k(t)$. If the signals $x_k(t)$ and $y_k(t)$ are approximately stationary in time, local time information can be ignored and instead global information can be utilized. As

*Laboratory of Information Processing, Lappeenranta University of Technology, P.O. Box 20, FIN-53851 Lappeenranta, Finland, [Joni.Kamarainen, Ville.Kyrki]@lut.fi.

†Laboratory of Electric Power Systems, Lappeenranta University of Technology, Tuomo.Lindh@lut.fi.

global information power spectra of the responses can be used

$$\int_{-\infty}^{\infty} |\psi(t) * x_k(t)|^2 dt \text{ and } \int_{-\infty}^{\infty} |\psi(t) * y_k(t)|^2 dt. \quad (1)$$

Due to the assumptions concerning the signals from two classes, the problem is restricted to the selection of type of the band-pass filter and values for the filter parameters, such as the central frequency f_ψ and the bandwidth ω_ψ .

2.1 Gabor filter

A Gabor filter can be used to form the bandpass filter ψ . A Gabor filter is defined as

$$\psi(t) = e^{-\alpha^2 t^2} e^{j(2\pi f_0 t)}. \quad (2)$$

In practice, the normalized form of the Gabor filter in the time domain

$$\psi(t) = \frac{f_0}{\sqrt{\pi}\gamma} e^{-(\frac{t_0}{\gamma})^2 t^2} e^{j(2\pi f_0 t)} \quad (3)$$

and in the frequency domain

$$\Psi(u) = e^{-(\frac{\pi\gamma}{f_0})^2 (u-f_0)^2} \quad (4)$$

are usually more convenient as feature extractors.

The reason for the normalization of the Gabor filters in (3) and (4) is to provide same convolution response regardless of the filter frequency f_0 . Now, the filtering parameters under consideration are the central frequency, controlled by f_0 , and the bandwidth, controlled by γ .

3 Filter-based signal discrimination

In this section discriminative energy functions are formed based on the first- and second-order statistics and the parameters of the Gabor filter are optimized by finding the argument values that maximize the energy functions providing the maximal discrimination.

3.1 First-order statistics based discrimination

If a dominant difference between two classes is the magnitude on some frequency band, first-order statistics can be used. Furthermore, if the signals are stationary over the time, the discrimination of classes can be done utilizing first-order statistics of the power spectra. The discrimination can be made using mean values of power spectra of filtered signals

$$\begin{aligned} \mu_x &= E_k \left\{ \int_{-\infty}^{\infty} |\psi(t) * x_k(t)|^2 dt \right\} \\ \mu_y &= E_k \left\{ \int_{-\infty}^{\infty} |\psi(t) * y_k(t)|^2 dt \right\}. \end{aligned} \quad (5)$$

Now, discrimination can be done calculating the Euclidean distance to the class mean values (5) and by assigning the class with the closest distance.

A special discrimination energy function can be formed to measure distances between the mean values of the two classes. The difference between mean values μ_x and μ_y can be defined as (one dimensional case)

$$E_1 = \frac{1}{2} (\mu_x - \mu_y)^2 \quad (6)$$

and the optimal filter parameters can be drawn from

$$\arg \max_{\gamma, f_0} E_1. \quad (7)$$

By utilizing the Parseval's energy conservation law and the Fourier convolution theorem the power spectrum equation can be rewritten

$$\int_{-\infty}^{\infty} |\psi(t) * x_k(t)|^2 dt = \int_{-\infty}^{\infty} |\Psi(u)X_k(u)|^2 du \quad (8)$$

where

$$\mathfrak{F}\{\psi(t)\} = \Psi(u) \text{ and } \mathfrak{F}\{x_k(t)\} = X_k(u). \quad (9)$$

Now, mean values in (5) can also be rewritten

$$\begin{aligned} \mu_x &= \frac{E}{k} \left\{ \int_{-\infty}^{\infty} |\Psi(u)X_k(u)|^2 du \right\} \\ \mu_y &= \frac{E}{k} \left\{ \int_{-\infty}^{\infty} |\Psi(u)Y_k(u)|^2 du \right\}. \end{aligned} \quad (10)$$

Because $\Psi(u)$ is always positive the above reduces to

$$\begin{aligned} \mu_x &= \frac{E}{k} \left\{ \int_{-\infty}^{\infty} \Psi^2(u)X_k(u)X_k^*(u) du \right\} \\ \mu_y &= \frac{E}{k} \left\{ \int_{-\infty}^{\infty} \Psi^2(u)Y_k(u)Y_k^*(u) du \right\}. \end{aligned} \quad (11)$$

In the discrete case the E_1 can be computed using equations

$$\begin{aligned} \mu_x &= \frac{1}{N_1} \sum_k \sum_u \Psi^2(u)X_k(u)X_k^*(u) \\ \mu_y &= \frac{1}{N_1} \sum_k \sum_u \Psi^2(u)Y_k(u)Y_k^*(u) \\ E_1 &= \frac{1}{2} (\mu_x - \mu_y)^2. \end{aligned} \quad (12)$$

3.1.1 Example

The signal discrimination based on first-order statistics of power spectra of filtered signals should be sufficient in the case of stationary signals with different amplitude content on some frequency band. If the frequency band is to be solved, then the discrimination energy function in (12) can be used to optimize

bandpass filter parameters. In this example the test signals were generated using following functions

$$\begin{aligned}
 x_k(t) &= \underbrace{A_n \text{normrand}(0, 1)}_{\text{noise}} + \underbrace{A_s \sin(2\pi \text{unifrand}(0, \frac{1}{2}) t)}_{\text{random sinusoid}} \\
 y_k(t) &= A_n \text{normrand}(0, 1) + A_s \sin(2\pi \text{unifrand}(0, \frac{1}{2}) t) + \underbrace{A_\alpha \sin(2\pi \text{normrand}(f_\alpha, \sigma_\alpha) t)}_{\text{class specific sinusoid}}, \quad (13)
 \end{aligned}$$

Where $\text{normrand}(\mu, \sigma)$ and $\text{unifrand}(a, b)$ generate normal or uniformly distributed random numbers with mean μ and deviation σ or from the interval $[a, b]$ respectively. Now, there is two discrete signal sets $x_k(t)$, $k = 0 \dots N_1 - 1$ and $y_k(t)$, $k = 0 \dots N_2 - 1$ for $t = 0 \dots N - 1$. Both signals contain Gaussian noise with deviation of amplitude A_n and uniformly distributed sinusoidal frequency components of amplitude A_s . Signal $y_k(t)$ contains also additional normal distributed frequency components concentrated on mean frequency f_α with deviation σ_α and amplitude A_α . Additional frequency components of $y_k(t)$ should be the most discriminative features to distinguish between two classes.

As shown in Fig. 1 the discrimination energy function (12) has its' maximum around the frequency $f_\alpha = 0.2$ (amplitude $A_\alpha = 1.0$ where the additional sinusoidal components in $y_k(t)$ are concentrated. In signal shown on the right-hand-side in Fig. 1 the amplitude of the additional frequency component in $y_k(t)$ is decreased ($A_\alpha = 0.5$) and due to thus weaker signal-noise-ratio the sufficient discriminative information is vanished and also the discriminative energy function is changed. Still, the correct maximum can be found.

3.2 Second-order statistics based discrimination

If there are several frequency bands where the classes C_1 and C_2 are dissimilar, then the band where the separation of classes is most evident should be selected. The first-order approach simply selects the frequency band where the distance between the mean values is largest, but neglects the variance information, and thus, a significant overlap of the classes may exist. Discrimination based on the second-order statistics provides a solution where probability distributions of magnitudes are as separate as possible. In the second-order approach the mean values μ_x and μ_y and variances σ_x^2 and σ_y^2 are needed along with some assumption of a form of the probability distribution $\phi(x)$.

As a standard statistical tool, the normal distribution can be used to represent the probability distributions of the data

$$\phi(n; \mu, \sigma^2) = \frac{1}{\sqrt{2\pi\sigma^2}} e^{-\frac{(n-\mu)^2}{2\sigma^2}} \quad (14)$$

As a measure of distribution similarity, the Kullback-Leibler divergence can be used

$$KL(\phi_1(n), \phi_2(n)) = \int_{-\infty}^{\infty} \phi_1(n) \log \frac{\phi_1(n)}{\phi_2(n)} dn \quad (15)$$

Now for discrete signals, equations for second-order statistics based discrimination are

$$\begin{aligned}
\mu_x &= \frac{1}{N_1} \sum_k \sum_u \Psi^2(u) X_k(u) X_k^*(u) \\
\mu_y &= \frac{1}{N_2} \sum_k \sum_u \Psi^2(u) Y_k(u) Y_k^*(u) \\
\sigma_x^2 &= \frac{1}{N_1 - 1} \sum_k \left[\sum_u \Psi^2(u) X_k(u) X_k^*(u) - \mu_x \right]^2 \\
\sigma_y^2 &= \frac{1}{N_2 - 1} \sum_k \left[\sum_u \Psi^2(u) Y_k(u) Y_k^*(u) - \mu_y \right]^2 \\
E_2 &= \frac{1}{2} \left(\int_{-\infty}^{\infty} \phi(n; \mu_x, \sigma_x^2) \log \frac{\phi(n; \mu_x, \sigma_x^2)}{\phi(n; \mu_y, \sigma_y^2)} dn \right)^2,
\end{aligned} \tag{16}$$

where numerical integration can be used to evaluate the actual value of E_2 (for example, the Lobatto quadrature provided by many scientific numerical computation softwares).

3.2.1 Example

Again in this example we consider discrete signals $x_k(t)$ from class C_1 and signals $y_k(t)$ from class C_2 . Both signals contain white noise with amplitude 0.1 and sinusoidal frequency components uniformly distributed between discrete frequencies 0 and 0.5 (0.5 is the Nyquist frequency) with amplitude 1.0. Both signals also contain additional sinusoidal frequencies centered at frequency 0.2 with deviation 0.05 and for class C_1 amplitude is 2.0 with deviation 2.0 and for class C_2 signals the amplitude is 4.0 with deviation 0.1 (significant overlap). Signals in the class C_2 also contain sinusoidal frequency components centered at frequency 0.35 with deviation 0.05 and amplitude 1.1 with deviation 0.1. The mean signals and their spectra and the discrimination energy functions E_1 and E_2 are shown in Fig. 2. From the energy functions it is clear that the E_1 has its maximum where the difference of mean magnitudes is largest ($f_0 = 0.2$) and E_2 where the distance between distributions is largest ($f_0 = 0.35$).

3.3 Optimizing filter parameters

For optimizing the filter parameters, gradients of the energy functions should be derived. The partial derivatives of the frequency domain Gabor filter function are

$$\begin{aligned}
\frac{\partial \Psi(u)}{\partial \gamma} &= \left(-\frac{2\pi^2 u^2 \gamma}{f_0^2} + \frac{4\pi^2 u \gamma}{f_0} - 2\pi^2 \gamma \right) e^{-(\frac{\pi \gamma}{f_0})^2 (u-f_0)^2} \\
\frac{\partial \Psi(u)}{\partial f_0} &= \left(\frac{2\pi^2 \gamma^2 u^2}{f_0^3} - \frac{2\pi^2 \gamma^2 u}{f_0^2} \right) e^{-(\frac{\pi \gamma}{f_0})^2 (u-f_0)^2}.
\end{aligned} \tag{17}$$

As one of the simplest optimizing methods of any partially differentiable discrimination energy function E , the steepest descent can be used for iterative

searching with learning factor μ

$$(\gamma_{t+1}, f_{0,t+1}) \leftarrow (\gamma_t, f_{0,t}) + \mu \left(\frac{\partial E}{\partial \gamma}, \frac{\partial E}{\partial f_0} \right). \quad (18)$$

However, it should be noted that with the basic gradient based methods, convergence to a local optimum will be more probable than convergence to the global one.

Optimizing E_1

$$\nabla E_1 = \left(\frac{\partial E_1}{\partial f_0}, \frac{\partial E_1}{\partial \gamma} \right) \quad (19)$$

where

$$\begin{aligned} \frac{\partial E_1}{\partial f_0} &= (\mu_x - \mu_y) \left[\frac{1}{N_1} \sum_k \sum_u 2\Psi(u) \frac{\partial \Psi(u)}{\partial f_0} X_k(u) X_k^*(u) - \right. \\ &\quad \left. \frac{1}{N_2} \sum_k \sum_u 2\Psi(u) \frac{\partial \Psi(u)}{\partial f_0} Y_k(u) Y_k^*(u) \right] \\ \frac{\partial E_1}{\partial \gamma} &= (\mu_x - \mu_y) \left[\frac{1}{N_1} \sum_k \sum_u 2\Psi(u) \frac{\partial \Psi(u)}{\partial \gamma} X_k(u) X_k^*(u) - \right. \\ &\quad \left. \frac{1}{N_2} \sum_k \sum_u 2\Psi(u) \frac{\partial \Psi(u)}{\partial \gamma} Y_k(u) Y_k^*(u) \right] \end{aligned} \quad (20)$$

As an example gradients of the same signals as in Fig. 1 are shown in Fig. 3. By comparing the left and right hand side images it can be seen that when the presence of discriminative information is less evident also the gradient information seems to be more unreliable. Also, one important feature is that the γ value controlling the bandwidth cannot necessarily be optimized but only the optimal central frequency f_0 can be optimized for given γ (see bottom images in Fig. 3).

Optimizing E_2

Similarly as with E_1 the partial differentiation and chain rule can be applied to construct a gradient

$$\nabla E_2 = \left(\frac{\partial E_2}{\partial f_0}, \frac{\partial E_2}{\partial \gamma} \right). \quad (21)$$

Following derivatives can be derived for the mean values in (16) utilizing also fast computations proposed later in (32)

$$\begin{aligned} \frac{\partial \mu_x}{\partial f_0} &= 2 \sum_u \Phi(u) \frac{\partial \Phi(u)}{\partial f_0} X(u) \\ \frac{\partial \mu_y}{\partial f_0} &= 2 \sum_u \Phi(u) \frac{\partial \Phi(u)}{\partial f_0} Y(u) \\ \frac{\partial \mu_x}{\partial \gamma} &= 2 \sum_u \Phi(u) \frac{\partial \Phi(u)}{\partial \gamma} X(u) \\ \frac{\partial \mu_y}{\partial \gamma} &= 2 \sum_u \Phi(u) \frac{\partial \Phi(u)}{\partial \gamma} Y(u) \end{aligned} \quad (22)$$

and for similarly partial derivatives of variances

$$\begin{aligned}
\frac{\partial \sigma_x^2}{\partial f_0} &= \frac{2}{N_1 - 1} \sum_k \left(\sum_u \Psi^2(u) X_k(u) X_k^*(u) - \mu_x \right) \\
&\quad \left(\sum_u 2\Psi(u) \frac{\partial \Psi(u)}{\partial f_0} X_k(u) X_k^*(u) - \frac{\partial \mu_x}{\partial f_0} \right) \\
\frac{\partial \sigma_x^2}{\partial \gamma} &= \frac{2}{N_1 - 1} \sum_k \left(\sum_u \Psi^2(u) X_k(u) X_k^*(u) - \mu_x \right) \\
&\quad \left(\sum_u 2\Psi(u) \frac{\partial \Psi(u)}{\partial \gamma} X_k(u) X_k^*(u) - \frac{\partial \mu_x}{\partial \gamma} \right) \\
\frac{\partial \sigma_y^2}{\partial f_0} &= \frac{2}{N_2 - 1} \sum_k \left(\sum_u \Psi^2(u) Y_k(u) Y_k^*(u) - \mu_y \right) \\
&\quad \left(\sum_u 2\Psi(u) \frac{\partial \Psi(u)}{\partial f_0} Y_k(u) Y_k^*(u) - \frac{\partial \mu_y}{\partial f_0} \right) \\
\frac{\partial \sigma_y^2}{\partial \gamma} &= \frac{2}{N_2 - 1} \sum_k \left(\sum_u \Psi^2(u) Y_k(u) Y_k^*(u) - \mu_y \right) \\
&\quad \left(\sum_u 2\Psi(u) \frac{\partial \Psi(u)}{\partial \gamma} Y_k(u) Y_k^*(u) - \frac{\partial \mu_y}{\partial \gamma} \right).
\end{aligned} \tag{23}$$

Now, by starting from the equation of E_2 defined in (16)

$$E_2 = \frac{1}{2} \left(\underbrace{\int_{-\infty}^{\infty} \phi(n; \mu_x, \sigma_x^2) \log \frac{\phi(n; \mu_x, \sigma_x^2)}{\phi(n; \mu_y, \sigma_y^2)} dn}_{E_2^{(1)}} \right)^2, \tag{24}$$

we may do partial derivatives

$$\begin{aligned}
\frac{\partial E_2}{\partial f_0} &= E_2^{(1)} \frac{\partial E_2^{(1)}}{\partial f_0} \\
\frac{\partial E_2}{\partial \gamma} &= E_2^{(1)} \frac{\partial E_2^{(1)}}{\partial \gamma},
\end{aligned} \tag{25}$$

where

$$\begin{aligned}
\frac{\partial E_2^{(1)}}{\partial f_0} &= \int_{-\infty}^{\infty} \frac{\partial \phi(n; \mu_x, \sigma_x^2)}{\partial f_0} E_2^{(2)} + \phi(n; \mu_x, \sigma_x^2) \frac{\partial E_2^{(2)}}{\partial f_0} dn \\
\frac{\partial E_2^{(1)}}{\partial \gamma} &= \int_{-\infty}^{\infty} \frac{\partial \phi(n; \mu_x, \sigma_x^2)}{\partial \gamma} E_2^{(2)} + \phi(n; \mu_x, \sigma_x^2) \frac{\partial E_2^{(2)}}{\partial \gamma} dn,
\end{aligned} \tag{26}$$

and because

$$E_2^{(2)} = \log \frac{\phi(n; \mu_x, \sigma_x^2)}{\phi(n; \mu_y, \sigma_y^2)} \tag{27}$$

is always real, then

$$\begin{aligned}\frac{\partial E_2^{(2)}}{\partial f_0} &= \frac{\frac{\partial \phi(n; \mu_x, \sigma_x^2)}{\partial f_0} \phi(n; \mu_y, \sigma_y^2) - \phi(n; \mu_x, \sigma_x^2) \frac{\partial \phi(n; \mu_y, \sigma_y^2)}{\partial f_0}}{\phi(n; \mu_x, \sigma_x^2) \phi(n; \mu_y, \sigma_y^2)} \\ \frac{\partial E_2^{(2)}}{\partial \gamma} &= \frac{\frac{\partial \phi(n; \mu_x, \sigma_x^2)}{\partial \gamma} \phi(n; \mu_y, \sigma_y^2) - \phi(n; \mu_x, \sigma_x^2) \frac{\partial \phi(n; \mu_y, \sigma_y^2)}{\partial \gamma}}{\phi(n; \mu_x, \sigma_x^2) \phi(n; \mu_y, \sigma_y^2)}.\end{aligned}\quad (28)$$

Finally, the partial derivatives of the probability distributions are needed

$$\begin{aligned}\phi(n; \mu, \sigma^2) &= \frac{1}{\underbrace{\sqrt{2\pi\sigma^2}}_{\phi^{(1)}}} \overbrace{e^{-\frac{(n-\mu)^2}{2\sigma^2}}}_{\phi^{(2)}} \\ \frac{\partial \phi(n; \mu, \sigma^2)}{\partial f_0} &= \frac{\partial \phi^{(1)}}{\partial f_0} \phi^{(2)} + \phi^{(1)} \frac{\partial \phi^{(2)}}{\partial f_0} \\ \frac{\partial \phi(n; \mu, \sigma^2)}{\partial \gamma} &= \frac{\partial \phi^{(1)}}{\partial \gamma} \phi^{(2)} + \phi^{(1)} \frac{\partial \phi^{(2)}}{\partial \gamma},\end{aligned}\quad (29)$$

where

$$\begin{aligned}\frac{\partial \phi^{(1)}}{\partial f_0} &= -\frac{1}{2\sqrt{2\pi}} (\sigma^2)^{-3/2} \frac{\partial \sigma^2}{\partial f_0} \\ \frac{\partial \phi^{(1)}}{\partial \gamma} &= -\frac{1}{2\sqrt{2\pi}} (\sigma^2)^{-3/2} \frac{\partial \sigma^2}{\partial \gamma} \\ \frac{\partial \phi^{(2)}}{\partial f_0} &= e^{-\frac{(n-\mu)^2}{2\sigma^2}} \frac{4(n-\mu) \frac{\partial \mu}{\partial f_0} \sigma^2 + 2(n-\mu)^2 \frac{\partial \sigma^2}{\partial f_0}}{4(\sigma^2)^2} \\ \frac{\partial \phi^{(2)}}{\partial \gamma} &= e^{-\frac{(n-\mu)^2}{2\sigma^2}} \frac{4(n-\mu) \frac{\partial \mu}{\partial \gamma} \sigma^2 + 2(n-\mu)^2 \frac{\partial \sigma^2}{\partial \gamma}}{4(\sigma^2)^2}\end{aligned}\quad (30)$$

For signals shown in Fig. 2, the gradients are computed (in Fig. 4 respectively). It is obvious that now the optimal values for f_0 and γ can be computed using the gradient information of E_2 .

4 Fast numerical computation of proposed algorithms

Computation of numerical values of the discrimination energy functions E_1 and E_2 in (12) and (16) may turn to a very time consuming if the number of signals (N_1 or N_2) or the length of the signals (N) are large. Some justifications can be made for computation of the discrimination energy functions.

Exact numerical values of the mean values μ_x and μ_y used by both, E_1 and E_2 , can be computed efficiently. It can be noted that the value of $\Psi(u)$ does not depend on k in calculation of μ_x and μ_y in (12) and (16). Thus, computation

of values

$$\begin{aligned}\frac{1}{N_1} \sum_k X_k(u) X_k^*(u) &= X(u) \\ \frac{1}{N_2} \sum_k Y_k(u) Y_k^*(u) &= Y(u)\end{aligned}\tag{31}$$

can be made in advance and now

$$\begin{aligned}\mu_x &= \sum_u \Psi^2(u) X(u) \\ \mu_y &= \sum_u \Psi^2(u) Y(u).\end{aligned}\tag{32}$$

Value of E_1 was computed using original (12) and fast method (32) and the results are shown in Fig. 1 where it is evident that the computation produces exactly the same numerical values (E1 exact, E1 fast).

The fast calculation of values of variances σ_x^2 and σ_y^2 in E_2 is more difficult because terms cannot be separated. However, the Gabor filter coefficients are close to zero elsewhere but near to the central frequency f_0 . Now, good estimate of the variance can be calculated by including only interval where the filter has at least some minimum response ϵ as

$$\begin{aligned}\sigma_x^2 &= \frac{1}{N_1 - 1} \sum_k \left[\sum_{u \in U_\epsilon} \Psi^2(u) X_k(u) X_k^*(u) - \mu_x \right]^2 \\ \sigma_y^2 &= \frac{1}{N_2 - 1} \sum_k \left[\sum_{u \in U_\epsilon} \Psi^2(u) Y_k(u) Y_k^*(u) - \mu_y \right]^2 \\ U_\epsilon &= \{u | \Psi(u) \geq \epsilon\}\end{aligned}\tag{33}$$

In Fig. 2(d) are shown the discrimination energy functions (E2 exact, E2 fast) calculated by exact computation (16) and by fast computation of variances (33).

5 Experiments

In this section, the methods presented are evaluated with the real-world problem of bearing condition monitoring of electric motors.

5.1 Background

The vibration analysis is the most important tool in the bearing condition monitoring of electric motors. On the other hand, a stator current measurement has an important role in finding many other faults of the induction motors. Unbalanced rotor, rotor bar damages, and damaged stator windings can be indicated with analyses based on the stator current measurement. The stator current measurement would be sufficient as the only condition monitoring "sensor" if bearing damages were found by analyses based on this measurement. Several studies have been published indicating that this could be possible. However, most of these have been made with very small motors. We present the experiments made with a 15 kW 4-pole induction motor.

When the geometry of a rolling bearing and a rotational speed of axle are known, the frequencies caused by bearing faults can be calculated. The characteristic frequency of the outer race defect of the bearing is calculated by equation

$$f_u = e \frac{N}{2} n_r \left(1 - \frac{d_b}{D} \cos \phi \right) \quad (34)$$

where N is the number of rolling elements, n_r is the rotational frequency, d_b is the diameter of the rolling element, D is the pitch diameter of bearing, ϕ is the contact angle between rolling element and race, and e is the ratio of rolling motion and slide, typically 0.96-0.98.

It has been shown, for example in [1], that the characteristic frequency of vibration caused by bearing defect is modulated to stator current frequency forming new current components at frequencies

$$f_{ib} = |f \pm m f_{vb}| \quad m = 1, 2, 3, \dots \quad (35)$$

where f is the frequency of the supply and f_{vb} is the frequency of vibration. When a ball of the bearing passes a defected spot on the race the clearance between inner and outer race grows allowing the rotor to move radially. This radial movement changes the air gap permeance inducing current to the stator. The force that moves the rotor radially is the unbalanced magnetic pull (UMP) caused by the combination of mechanical and magnetic asymmetries. The rotating air gap flux wave causes the modulation to the induced current. The results presented earlier in [2] indicate that the bearing faults can be detected by using stator current measurement only if the internal radial clearance of bearing is large.

5.2 Classification experiment

The data set consisted of stator current signals measured from motors from two classes: motors in normal condition and motors with bearing damage. There were 7 measurement sets measured from motors in normal condition and 9 sets from motors with a bearing damage. All sets contained 40 measurements where signals were recorded 11.0 seconds with sampling frequency $f_s = 3000$ Hz. In the experiment the frequency bands were inspected using Gabor filters on different central frequencies f_0 and bandwidth $\gamma = 8.0$. For classification of signals a Bayesian classifier was used and the experiment was conducted using leave one measurement set out method. In Fig. 5 are shown the classification accuracy of the Bayesian classifier with filtered signals and filters on different frequencies, and the discrimination energy functions E_1 and E_2 . The best classification results were achieved on frequencies where the E_2 had maxima (see Fig. 5). E_1 did not seem to present information about the discrimination efficiency of frequencies.

5.3 Practical evaluation

Now, the experimental results are analysed based on former knowledge [1, 2]. In the measurements, all conditions except the damage of the bearing were kept as constant as possible. Under this condition, we can hypothesise that if the bearing damage changes the frequency components of the stator current, the

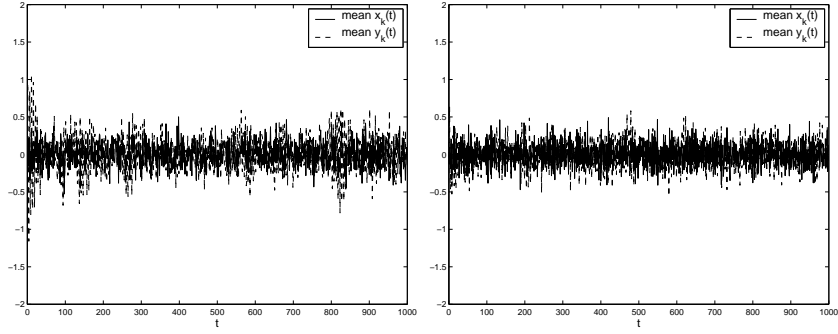
difference between healthy and broken case signals should be bigger on these frequencies than on any other frequencies. This can be tested by using the E_2 measure introduced in this report. If not, the expectations of equations (34) and (35) are not correct, and the frequency content change at these frequencies is smaller than coincidental changes caused by small mechanical load variations or other unknown sources. In this experiment, the bandwidth of filter was reduced by setting $\gamma = 16$ to have more visible peaks in the discrimination.

The results of the optimisation are presented in Figures 6–8. Figure 6 presents the discrimination energy E_2 between the signals measured in the cases of healthy and broken bearing when the motor was equipped with the bearings with normal internal radial clearance. The E_2 has the peak value at the frequency near 600 Hz. The peak is not near the modulated bearing frequencies and the fact that there is only one peak indicates that it is not originated from bearing pass impulse. On the other hand, the amplitude of the peak is much higher than in the case where two measurements from healthy case are compared. This difference remains inexplicable (no explanatory factor was found).

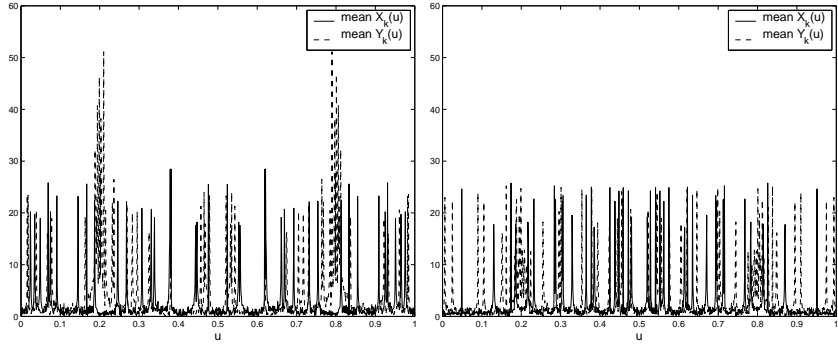
The discrimination energy E_2 was calculated also between signals measured in the cases where the motor was equipped with the bearings of larger internal radial clearance. The difference between results of two measurement sets from the healthy bearing (Fig. 7) and the results where healthy bearing case was compared to the broken bearing case is significant (Fig. 8). The peaks were found near calculated frequencies and, as expected, the peaks were repeated with intervals of the bearing pass frequency. The results clearly support the results presented in [2] where the bearing damages could be found and classified reliably in the where the motor was equipped with the bearings with the large internal clearance. The results also indicate that the discrimination energy E_2 can find the most significant differences in the frequency spectra of signals even if the changes are very faint. First-Order statistics (E_1) were found to find the harmonic frequencies of supply due to normal slight variation of motor load. As a conclusion, the outer race defect was clearly indicated only in the case of the large internal radial clearance of the bearing.

REFERENCES

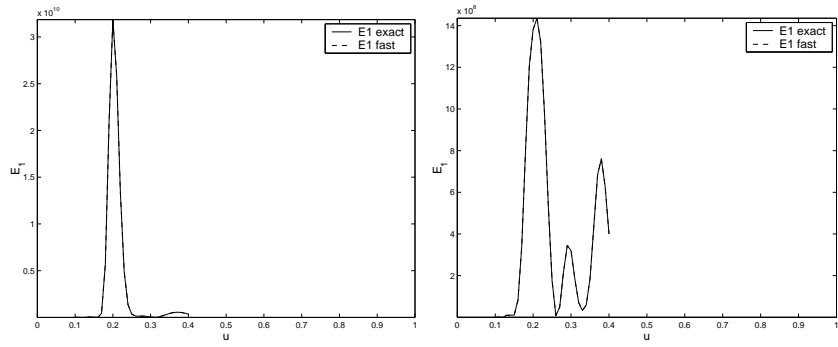
- [1] R. R. Schoen, T. G. Habetler, F. Kamran, and R. G. Bartfield, “Motor bearing damage detection using stator current monitoring,” *IEEE Transactions on Industry Applications*, vol. 31, no. 6, pp. 1274–1279, 1995.
- [2] T. Lindh, J. Ahola, and J. Partanen, “An evaluation of condition monitoring of bearings of 15 kw induction motor based on stator current measurement,” in *ICEM 2002*, (Bruges, Belgium), August 26–28 2002.



(a) Mean signals

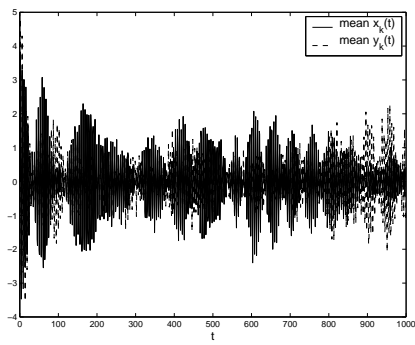


(b) Mean spectra

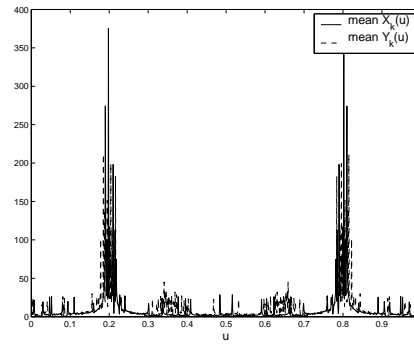


(c) E_1

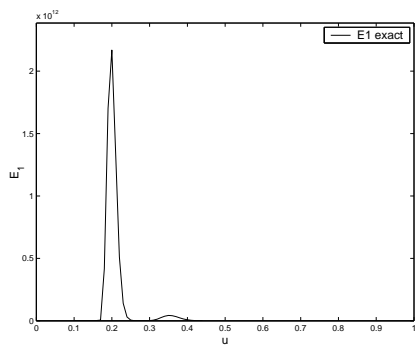
Figure 1: Signals, spectra and discrimination energy functions ($A_n = 0.1$, $A_s = 1$, $A_\alpha = \{1, 0.5\}$, $f_\alpha = 0.2$, $\sigma_\alpha = 0.05$).



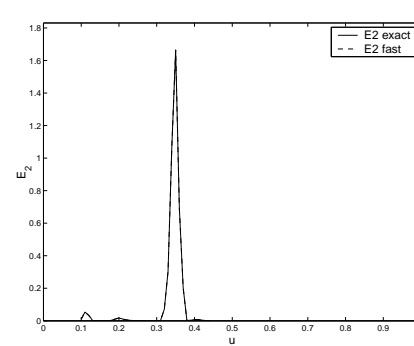
(a) Mean signals



(b) Mean spectra

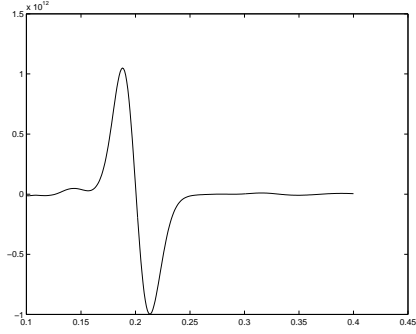


(c) E1

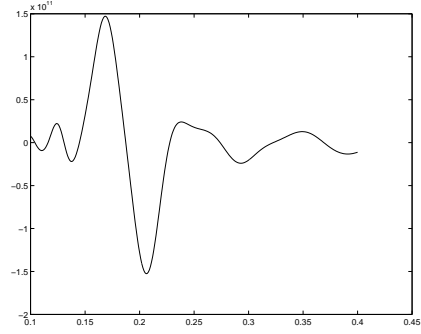


(d) E2

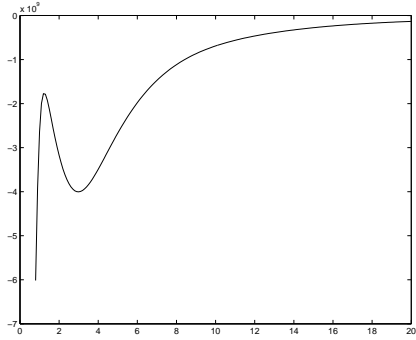
Figure 2: Signals, spectra, and discrimination energy functions.



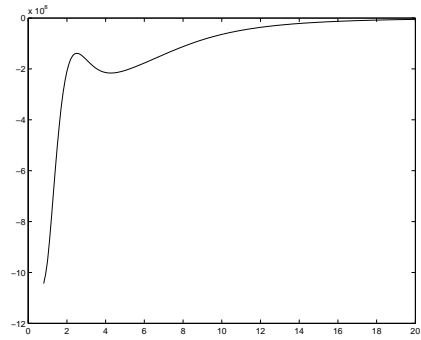
(a) $\partial E_1 / \partial f_0, \gamma = 2$



(b) $\partial E_1 / \partial f_0, \gamma = 2$

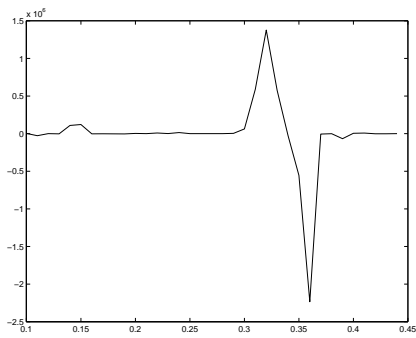


(c) $\partial E_1 / \partial \gamma, f_0 = 0.2$

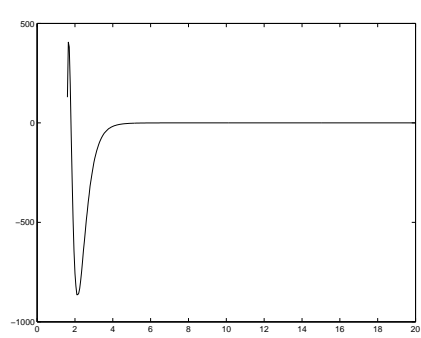


(d) $\partial E_1 / \partial \gamma, f_0 = 0.18$

Figure 3: Gradients of discrimination energy function E_1 .

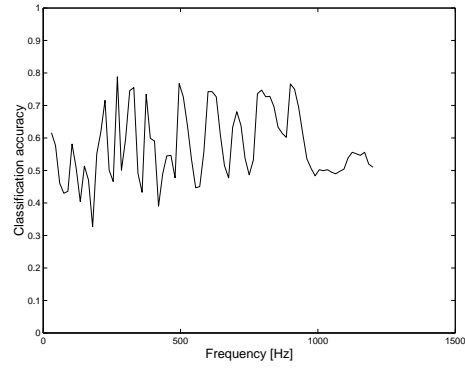


(a) $\partial E_2 / \partial f_0$ for $\gamma = 4.0$

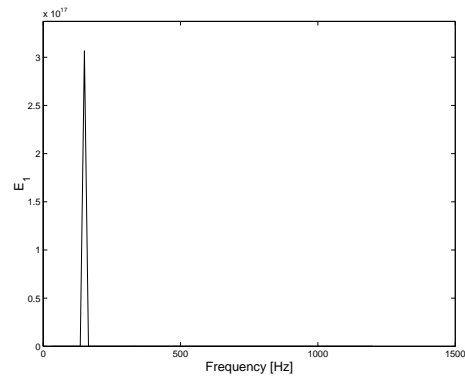


(b) $\partial E_2 / \partial \gamma$ for $f_0 = 0.35$

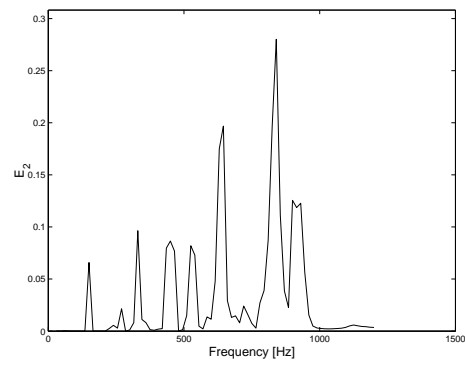
Figure 4: Gradients of discrimination energy function E_2 .



(a) Classification accuracy



(b) E_1 discrimination energy



(c) E_2 discrimination energy

Figure 5: Classification results and discrimination energy functions for SMOOTT01 data set.

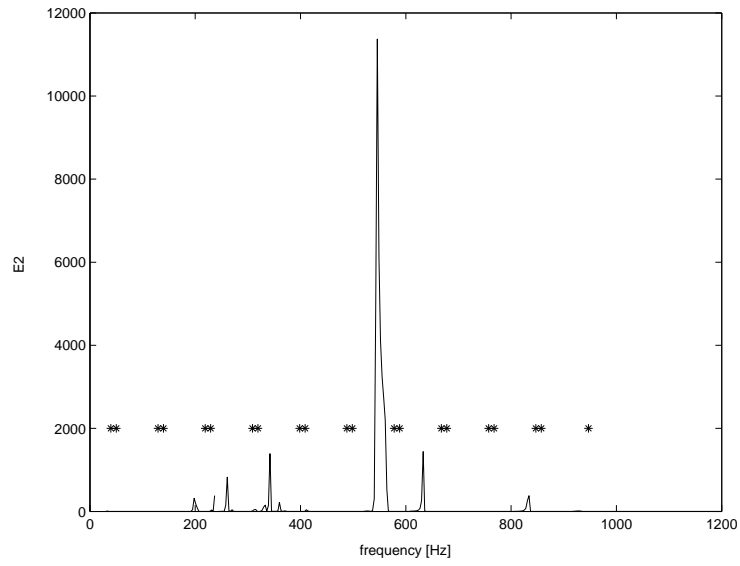


Figure 6: Discrimination energy E_2 on different frequencies, healthy and broken bearings with normal clearance. Asterisks denote the supposed characteristic frequencies.

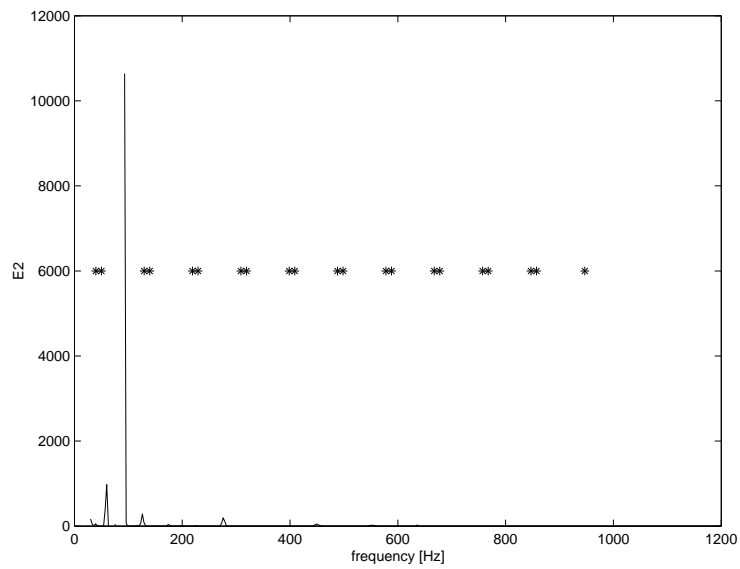


Figure 7: Discrimination energy E_2 on different frequencies, two sets of healthy bearings with large clearance. Asterisks denote the supposed characteristic frequencies.

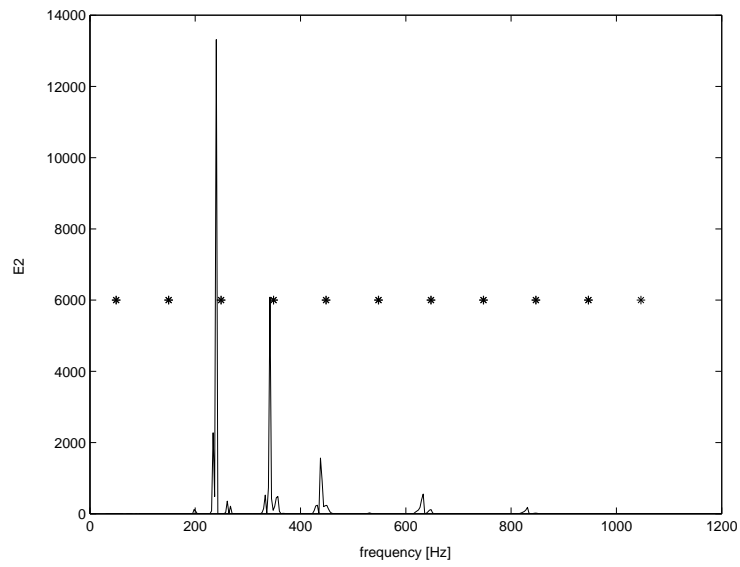


Figure 8: Discrimination energy E_2 on different frequencies, healthy and broken bearings with large clearance. Asterisks denote the supposed characteristic frequencies.